

Tu LHR5 14

## Use of Ambient Noise to Enhance Low Frequencies Seismic Migration Images

B. De Cacqueray\* (CGG), J. Cotton (CGG), F. Duret (CGG), C. Berron (CGG)  
& E. Forgues (CGG)

### SUMMARY

---

In this study, we propose an example of body wave retrieval using ambient noise correlation. The correlated data are migrated using a Kirchhoff pre-stack time migration (PSTM) and then with the migration obtained with conventional active data. It allows to considerably broaden the final image spectrum toward the low frequencies.

## Introduction

Using ambient noise correlations, Green's function between two receivers can be recovered (Campillo and Paul, 2003). Due to their higher energy, surface waves are easier to retrieve than body waves (Wapenaar and Fokkema, 2006) and can be even used for 4D tomography (Duret and Forgues). However, using correlation, Draganov et al. (2009) succeeded in imaging the subsurface in the context of seismic exploration while Poli et al. (2012) demonstrated that the recovery of body waves is feasible at the seismology's scale.

For seismic exploration (i.e. reservoir geophysics), retrieval of body waves appears promising, especially at low frequencies (below 3 Hz) where seismic vibrators reach a limit. These low frequencies are of interest for velocity model building (Baeten et al. 2013) and for broadband seismic inversion (Kneller et al. 2014).

Here we demonstrate an example of body wave retrieval using ambient noise correlation in the context of seismic monitoring. The result of the ambient noise correlation is correctly arranged to produce noise-induced shot point gathers at each sensor positions. The numerous noise-induced shot point gathers are then migrated using a Kirchhoff pre-stack time migration (PSTM) method in order to obtain a noise-induced image of the subsurface. The noise-induced migrated image is compared and then combined with the image obtained by migrating the conventional active shot point gathers generated by vibroseismic sources (Cotton et al, 2014). In so doing, we considerably broaden the image spectrum toward the low frequencies.

## Acquisition design and method

Ambient noise correlation states that correlating the signals of two receivers recording random ambient noise allows reconstruction of the Green's function (i.e. the "Earth's response") between both receivers, as if a source were placed at one of the two receivers.

Although the exact reconstruction of the Green's function requires homogenous distribution of the ambient noise sources around the two receivers, it has been shown that a good enough proxy of the Green's function can be obtained with more restricted source distribution (de Cacqueray, 2012). This is the case when ambient noise sources are more or less aligned with the two receivers as illustrated in *Figure 1*. In these configurations, surface wave reconstruction appears easier as having ambient noise sources at the surface is relatively common. For body wave reflection, the ambient noise signal has to travel in a more complex way (dotted arrows in *Figure 1*, bottom). In the case of the location of deep ambient noise sources (dark blue in *Figure 1*, bottom) travel paths result in lower attenuation.

In this study, real reflection seismic data are used. The onshore acquisition configuration comprises 57 permanent sources buried at a depth of 25 m and 1350 hydrophones buried at a depth of 20 m, covering a 1.8 km<sup>2</sup> area. In the area of interest, the imaging target area is a thin (~25 m) reservoir at a depth of ~550 m (0.5 s TWT). The description of the acquisition is available in Lopez et al. (2015).

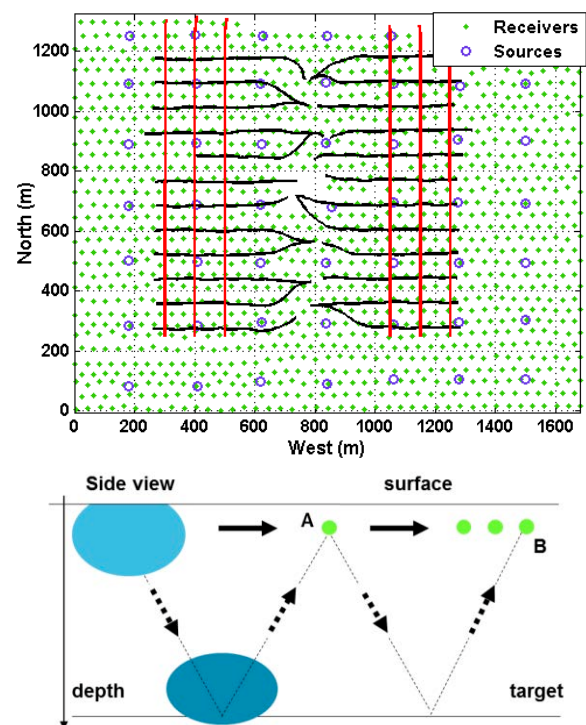


**Figure 1** Top: view of the acquisition spread with (green) buried hydrophones (blue), buried controlled sources (black) production wells (red), injectors wells.

Bottom: (bluish areas) favourable ambient noise sources location for (plain arrows) surface wave reconstruction and (dotted arrows) body wave reconstruction between A and B.

## Noise correlation and shot gather arrangement

The time-frequency representation of a 30-min recorded signal at a receiver is displayed in

*Figure 2*. Different types of signals are visible: i) the controlled source signal in the white ellipse, ii) strong mono frequency (electrical signal and sub-harmonic) at 60 Hz and 30 Hz, iii) anthropic noise (inside purple and yellow ellipses). In the [30-60] Hz bandwidth, the ambient noise shows intermittences (inside yellow ellipse) that suggest anthropic activities. We observe that the amplitude of the active signal decreases in the low frequencies whereas the amplitude of the ambient noise is strong. Such ambient noise predominance and intensity supports the case for using it for imaging through correlation.

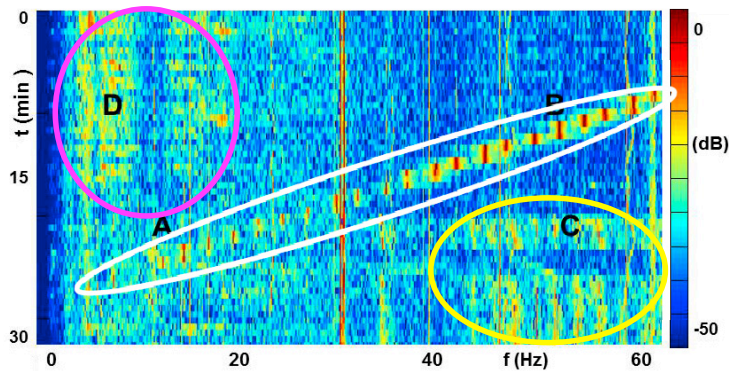


**Figure 2** Time-Frequency zoom on a [0-60] Hz frequency band for 30-min recording by one buried hydrophone.

Energy in the white ellipse comes from the emitted mono frequency controlled signal.

The purple and yellow ellipse areas correspond to anthropic sources of noise that generate surface and body waves.

In order to correlate only ambient noise, the controlled signal is removed using a simple difference of two consecutive records. Due to the system's high repeatability (Berron et al. 2015) the controlled signal's day-to-day difference is close to zero so that the daily difference of the full record is only the difference between two ambient noise records.

For six-hour long records, about 225,000 correlations of 20 s have been computed between sensors using a selection of 672 buried hydrophones (every 2<sup>nd</sup> hydrophone of *Figure 1*). Each correlation between two receivers A and B provides signal in both causal and acausal times. The causal part is the signal that would be emitted by a virtual source at position A for a receiver at position B, the other part, in the acausal time, provides the signal emitted by a virtual source at position B and a receiver at position A. Causal and acausal times can be combined to obtain more than 450 000 correlated traces of 10 s, which are then downsampled to 10 ms as we are interested only in the low-frequency bandwidth. A single 12 cores computer can correlate one hour of continuous data in less than 25 min, so that correlations can be performed on site in real-time.

The result of the ambient noise correlation is correctly arranged to produce induced shotpoint gathers at each sensor position. *Figure 3* illustrates the comparison between the conventional shotpoint gathers generated by a vibroseismic source and the induced shot point. The first arrivals for P waves appear in both cases. The reservoir reflection is expected around time 0.5 s. It is visible at all offsets for the active data and appears at several offsets on the correlated data.

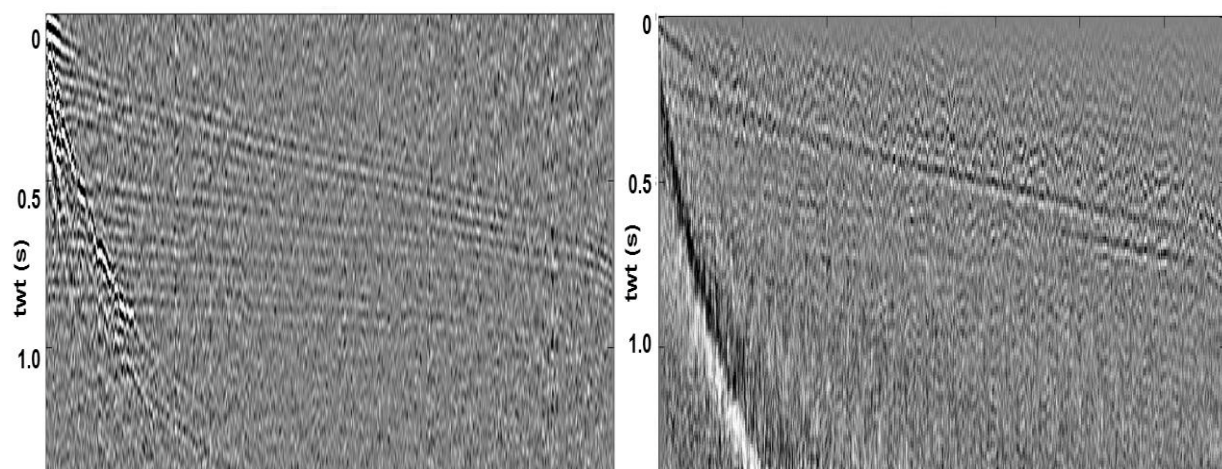


**Figure 3** Shot gathers in the [0-25] Hz frequency band for a controlled active source summed over 24 h (left) and ambient noise correlation summed over 6 h (right).

## PSTM and spectrum broadening with ambient noise correlations

Using a 1D velocity model, a 3D Pre-Stack Time Migration (PSTM) has been performed on both correlated data and controlled source data. *Figure 4* presents migrations up to 2.5 s TWT for three frequency bands: [0-25], [0-5] and [0-1.5] Hz. In the first case (*Figure 4 a, b*), reflections at 0.5 s (reservoir), 0.67 s, 0.8 s, 1.5 s and 2 s are visible for both methods. In the [0-5] Hz frequency band, ambient noise correlations better image the reflections around 0,3, 1.5 and 2,2 s while controlled active sources give better signal around 1 and 2 s (*Figure 4 c, d*). Below 1.5 Hz, our emitted signal is very weak, so that only the correlated data result seems usable. This underlines the coherency (medium frequencies) and the complementarity (low frequencies) of both results and suggests the value of merging of the two datasets (patent Cotton et al. 2014). *Figure 5* highlights the broadening of the low-frequency spectrum of the active dataset thanks to ambient noise correlated data.

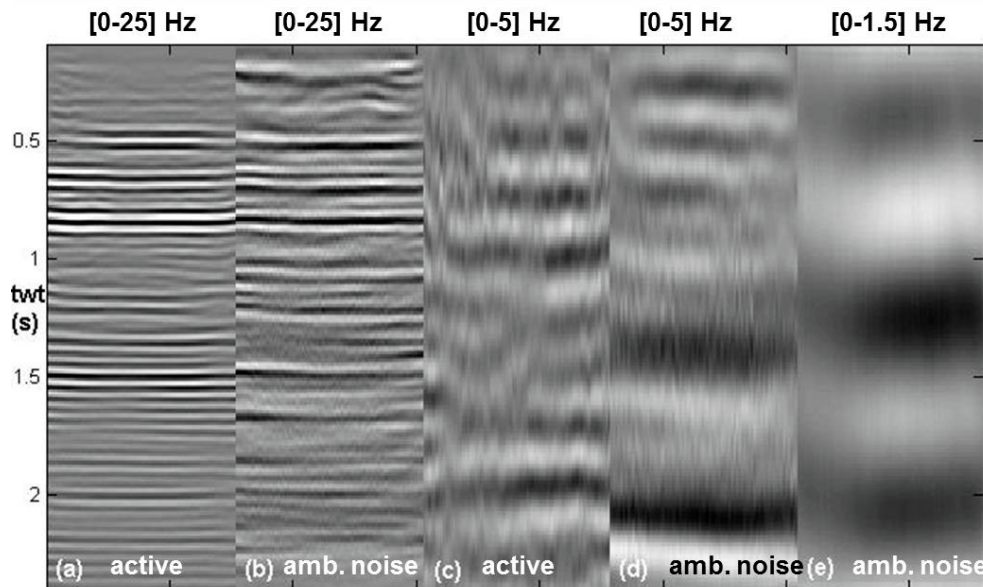


**Figure 4** The same PSTM section from controlled sources (a, c) and ambient noise correlations (b, d, e), for different frequency bands. Different gains are applied for display.

Ambient noise correlation brings low-frequency information.

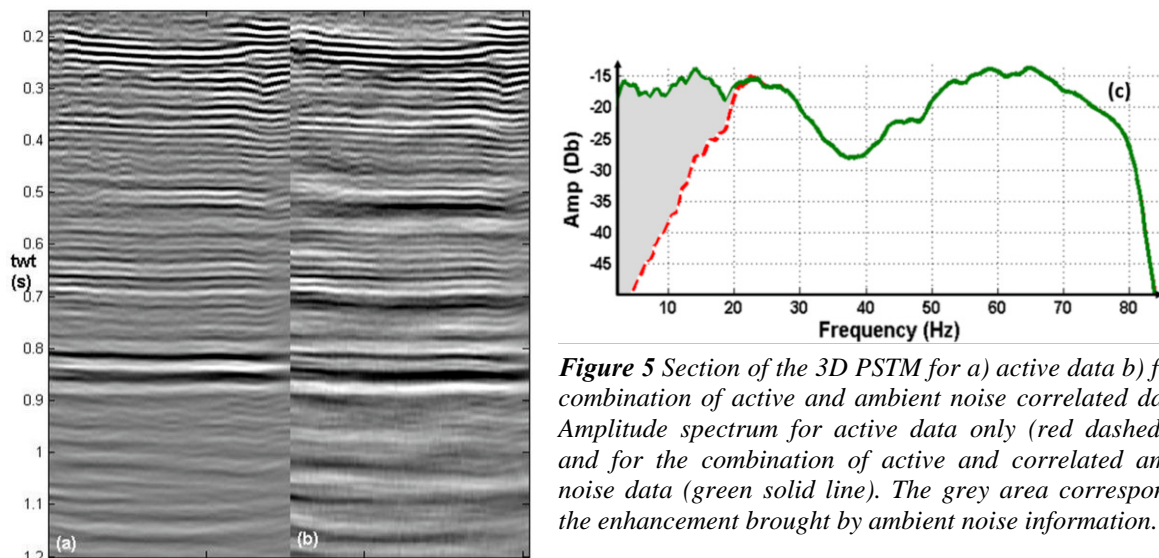


**Figure 5** Section of the 3D PSTM for a) active data b) for the combination of active and ambient noise correlated data. c) Amplitude spectrum for active data only (red dashed line) and for the combination of active and correlated ambient noise data (green solid line). The grey area corresponds to the enhancement brought by ambient noise information.

## Conclusion

In this study, it is shown that ambient noise correlations can be used to properly recover body wave reflections for use in seismic imaging, providing that sources of ambient noise are available with enough energy and/or permanency. Depending on this noise level and giving preference to continuous recording, this approach opens the door for merging ambient noise correlations and conventional 3D data in order to bring low frequencies into the final subsurface image.

## Acknowledgements

We would like to thank Shell for kindly allowing us to use the data and present the results.

## References

- Baeten, G., de Maag J.M., Plessix R.E., Klaassen, R., Qureshi, T., Kleemeyer, M., ten Kroode F., Rujie Z. [2013] The use of low frequencies in a FWI and impedance inversion land seismic case study. *Geophysical Prospecting*, **61**, 701-711.
- Berron C., Michou L., de Cacqueray B., Duret F., Cotton J., Forgues E., Winter O. [2015] Permanent, continuous & unmanned 4D seismic monitoring: Peace River case study. *SEG 85<sup>th</sup> Annual Meeting*, New Orleans.
- Campillo, M. and Paul, A. [2003] Long range correlations in the diffusive seismic coda. *Sciences*, **299**, 547-549.
- Cotton, J., Duret, F., Forgues, E. [2014] Combination of controlled and uncontrolled seismic data. *CGG PCT WO2015/124961*.
- de Cacqueray, B. [2012] *Dispositifs géophysiques à l'échelle du laboratoire*. PhD Thesis, Université Joseph Fourier.
- Draganov, D., Campman, X., Thorbecke, J., Verdel A. Wapenaar K. [2009] Reflection images from ambient seismic noise. *Geophysics*, **74**, 5.
- Duret F, and Forgues, E. [2015] 4D Surface Wave Tomography Using Ambient Seismic Noise. *77<sup>th</sup> EAGE Conference and Exhibition*, Madrid, Spain
- Kneller E., Zekian L., Coleou T., Coulon J.P., Lafet. Y. [2014] Benefits of Broadband Seismic Data for Reservoir Characterization - Santos Basin, Brasil. *76<sup>th</sup> EAGE Conference and Exhibition*, Amsterdam.
- Lopez, J.L., P.B. Wills, J.R. La Follett, T.B. Barker, Y. Xue, J.K. Przybysz-Jarnut, M. Van Lokven, R., R. Brouwer, and C. Berron, [2015] Real-time seismic surveillance of thermal EOR at Peace River. Canada Heavy Oil Technical Conference, Society of Petroleum Engineers, Paper SPE-174459-M.
- Poli P., Campillo M., Pedersen H. and the Lapnet Working Group, [2012] Body wave imaging of the Earth's mantle discontinuities from ambient seismic noise. *Science*, **338**, 1063-1066.
- Wapenaar, K. and Fokkema, J. [2006] Green's function representations for seismic interferometry. *Geophysics*, **71**(4).